Supporting Information

# Design and Synthesis of Single-Benzene-Based Fluorophores with Red/NIR Emission for Dual-Function Optical Waveguides and Photodynamic Therapy

*Jianan Dai,* [a,b] *Xuan Wang,* [a,b] *Zhuolin Zhan,* [a,b] *Chunyu Wei,* [a] *Yuan Chai,* [a,b] *Jie Hua,* [a,b] *He Dong,* [a,b] *Guofeng Wang,* [a,b] *Jin Wang,* [a,b*] *Jing Liu* [c*] *and Laiping Fang* [d*]

[a] College of Information Technology, Jilin Engineering Research Center of Optoelectronic Materials and Devices, Jilin Normal University, Siping 136000, China.

[b] Jilin Provincial Key Laboratory of Wide Bandgap Semiconductor Material Growth and Device Applications, Jilin Normal University, Changchun 130103, China.

[c] Department of Chemical Physics, University of Science and Technology of China, Hefei 230022, China

[d] Guangdong Second Provincial General Hospital, School of Medicine, Jinan University, Guangzhou 518037, China.

# Contents

## 1. Chemical Synthesis

**General**. $^1$H NMR spectra were recorded with a Bruker AVENCE III HD 400 M in $CDCl_3$-d. The chemical shifts in $^1$H NMR spectra were reported in $\delta$ ppm using tetramethylsilane as an internal standard. All reactions were performed under a $N_2$ atmosphere, unless otherwise stated. Commercially available solvents and reagents were used without further purification unless otherwise mentioned. wx-2 was synthesized according to the literatures. [1]

**wx-1**. To the solids of dimethyl 2,5-dibromoterephthalaldehyde (0.80 g, 2.74 mmol), RuPhos (350 mg, 0.750 mmol), $Pd_2(dba)_3$ (140 mg, 0.153 mmol), and $Cs_2CO_3$ (13.03 g, 40.0 mmol) were added toluene (20 mL) and piperidine (1.17 g, 13.7 mmol), successively, and the resulting mixture was stirred at 120 °C for 12 h. After cooling to room temperature, EtOAC (50 mL) and water (20 mL) were added to the mixture. After separation, the organic layer was washed with water (20 mL) and brine (20 mL), and then dried over anhydrous $Na_2SO_4$, and filtered. After concentration of the filtrate under reduced pressure, the resulting solid was purified by silica gel column chromatography to afford 80 mg of wx-1 as red solids. $^1$H NMR (400 MHz, Chloroform-*d*, δ): 10.36 (s, 2H), 7.56 (s, 2H), 3.01 (t, $J$ = 5.3 Hz, 8H), 1.81 – 1.69 (m, 8H), 1.64 – 1.56 (m, 4H).

**wx-2**. $^1$H NMR (400 MHz, Chloroform-*d*, δ): 9.76 (s, 1H), 7.74 (d, $J$ = 8.8 Hz, 2H), 6.95 (d, $J$ = 6.2 Hz, 2H), 3.41 (d, $J$ = 5.5 Hz, 4H), 1.69 (s, 6H).

## 2. Photophysical Properties

**Measurements**. UV-vis absorption spectra of solutions were measured with a SHIMADZU UV-2700 UV-VIS SPECTROPHOTOMETER. Emission spectra of solutions and solids were measured with an Ocean QE Pro fibre optic spectrometer. Absolute fluorescence quantum yields ($\Phi_F$) of solutions and crystal were determined with an Ocean QE Pro fibre optic spectrometer equipped with a calibrated integrating sphere system.

## 3. Experimental Details of Theoretical Calculations

**Methods**. The time-dependent density functional theory (TD-DFT) calculation was performed using Gaussian 16 program at the B3LYP/6-31G* level of theory. Reorganization energy analysis of all molecules was performed using the MOMAP 2022B.

## 4. X-ray Crystallographic Analysis

**Single crystal X-ray measurements**. Single crystal X-ray diffraction data were collected on a Bruker SMART ApeX II using the $\omega$-scan mode with graphite monochromator Mo•Kα radiation. The structures were solved with direct methods using the SHELXTL programs and refined with full-matrix least-squares on $F^2$. Non-hydrogen atoms were refined anisotropically. The positions of hydrogen atoms were calculated and refined isotropically. Crystals of polymorph A was were obtained by liquid/liquid diffusion of its $CH_2Cl_2$ solution and petroleum ether at room temperature. Crystals of polymorph B was obtained by liquid/liquid diffusion of its $CH_2Cl_2$ solution and methanol at room temperature. The crystal structures have been deposited with the Cambridge Crystallographic Data Centre (polymorph A: CCDC 2389721; polymorph B: CCDC 2389717).

## 5. Optical waveguide properties Measurements

The crystal was irradiated by the third harmonic (355 nm) of a Nd:YAG (yttriumaluminum-garnet) laser at a repetition rate of 10 Hz and a pulse duration of about 10 ns. The energy of laser was adjusted by using the calibrated neutral density filters. The beam was focused into a stripe whose shape was adjusted to 3.3 × 0.6 mm by using[1] a cylindrical lens and a slit. The emission was detected at one end of the crystal using a Maya 2000 Pro CCD spectrometer.

## 6. Detection of Overall ROS Generation

Under the irradiation of white light, using 2, 7-ichlorodihydrofluorescein (DCFH) as

the indicator, and the ROS generation measurements of wx-1 were conducted. After the reaction for 30 min in the dark in DCFH-DA (1 mL, 2 mM) with NaOH solution (9 mL, 10 mM), 30 mL of PBS buffer solution was then added to the reaction mixture to obtain DCFH solution with a concentration of 50 μM. Afterward, 1 mL DCFH solution (10 μM) and 100 μL of wx-1 (500 μM) were added in 4 mL of PBS. Finally, the mixture of 2 μM DCFH and 10 μM wx-1 was obtained under vigorous stirring. The PL spectra were collected before and after white light exposure at different irradiation times. The fluorescence intensity at 525 nm was recorded to indicate the ROS generation.

**7. Detection of $^1O_2$ by DPBF**

To further distinguish the type of ROS generated by wx-1, DPBF was used to evaluate the singlet oxygen generation ability under white light irradiation. In brief, 2.7 mg DPBF dissolved in 1 mL DMSO. During testing, 100 uL of wx-1 (500 uM), 20 uL of DPBF solution and 3 mL of DMSO were mixed well, and then exposed to white light irradiation. The absorbance decrease of DPBF at 415 nm was recorded after various irradiation times.

**8. Detection of $O_2^{-\cdot}$ by DHR123**

DHR123 was employed to assess the $O_2^{-\cdot}$ generation ability under white light irradiation. In brief, DHR123 (5 μM) and wx-1 (2 μM) in DMSO were mixed and then exposed to white light irradiation. The fluorescence peak at 526 nm was recorded after various irradiation times.

**9. Detection of ·OH by HPF**

HPF was utilized to estimate the ·OH generation ability under white light irradiation. In brief, HPF (5 μM) and wx-1 (2 μM) in DMSO were mixed and then exposed to white light irradiation. The fluorescence peak at 515 nm was recorded after various irradiation times.

## 10. Biocompatibility and Phototoxicity Assay

The biocompatibility and toxicity of wx-1 were studied by using the standard CCK-8 assay. EMT6 cells were added in 96-well plates ($5 \times 10^3$ cells/well). After incubation for 24 hours, the cells were cultured with wx-1 by different concentrations for 12 hours. The EMT6 cells in the irradiation group were illuminated for 15 minutes by white light (100 mW $cm^{-2}$). Meanwhile, the wx-1 incubated cells without irradiation were also conducted to explore the biocompatibility. After further incubation for 12 hours, the medium was removed and washed with PBS three times. The standard CCK-8 test was carried out.

## 11. Intracellular ROS Generation

The intracellular production of ROS was detected by DCFH-DA. EMT6 cells were incubated with wx-1 (50 μg $mL^{-1}$) for 12 hours. Then, the cells were washed and replaced with fresh medium. Subsequently, 10 μM DCFH-DA was added into a Petri dish and cultured for 20 minutes in the incubator. Afterward, the cells were illuminated by a white light for 15 minutes (100 mW $cm^{-2}$). After 3 hours, the cells were imaged by fluorescence microscope.

## 12. Live-Dead Cell Staining

The EMT6 cells were seeded and cultured in a glass bottom dish for 24 hours, wx-1 (50 μg $mL^{-1}$) were then added into the cell culture medium. After 12 hours of incubation, the cells were washed and replaced with fresh medium, followed by white light irradiation (100 mW $cm^{-2}$) for 15 minutes. After that, the cells were incubated at 37 $^{o}$C for another 1 h, then successively stained with PI and Calcein AM in PBS for 10 minutes. Subsequently, the cells were gently washed and then imaged by fluorescence microscope.

## 13. Supporting Schemes, Figures and Tables

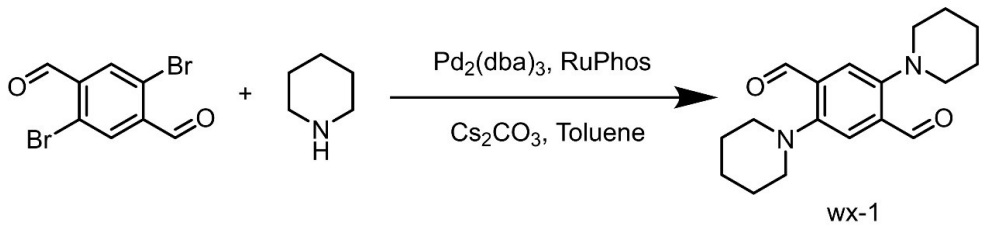


**Scheme S1**. Synthesis of wx-1

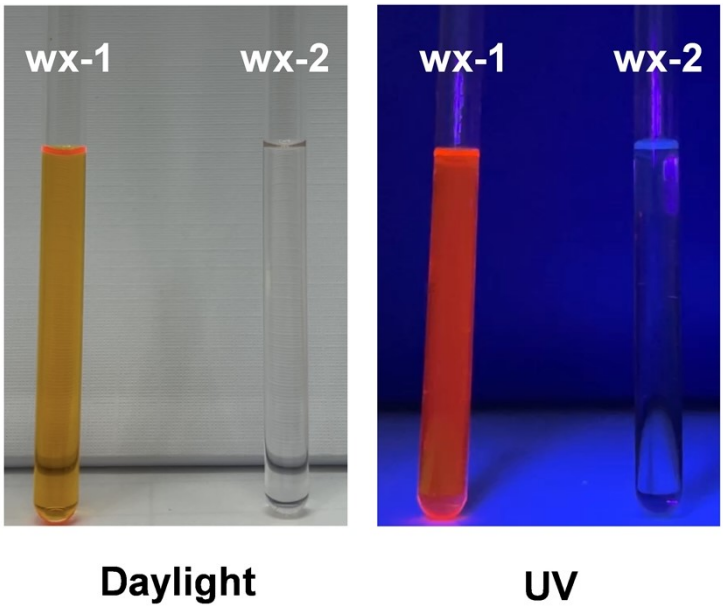


**Figure S1**. Photographs of wx-1 and wx-2 in toluene solution (under daylight and UV irradiation).

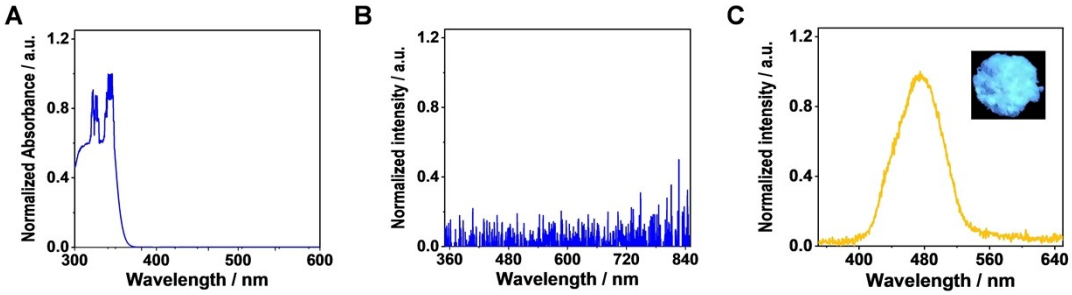


**Figure S2**. (A) Normalized absorbance spectra of wx-2 in toluene solution. (B) Normalized fluorescence spectra of wx-2 in toluene solution. (C) Normalized fluorescence spectra of wx-2 solid powder. The inset is digital photograph of wx-2 in solid powder under UV irradiation.

**Table S1.** Photophysical Data for wx-1 in solution and the crystalline states

| Solvent | $\lambda_{abs}$ / nm | $\lambda_{em}$ / nm | $\Phi_F$ / %[a] |
|---|---|---|---|
| toluene | 453 | 621 | 25.6 |
| $CHCl_3$ | 460 | 669 | 7.3 |
| DCM | 460 | 655 | 14.7 |
| DMF | 457 | 657 | 9.23 |
| polymorph A | | 600 | 7 |
| polymorph B | | 657 | 12 |

[a] Absolute fluorescence quantum yield determined by a calibrated integrating sphere system.

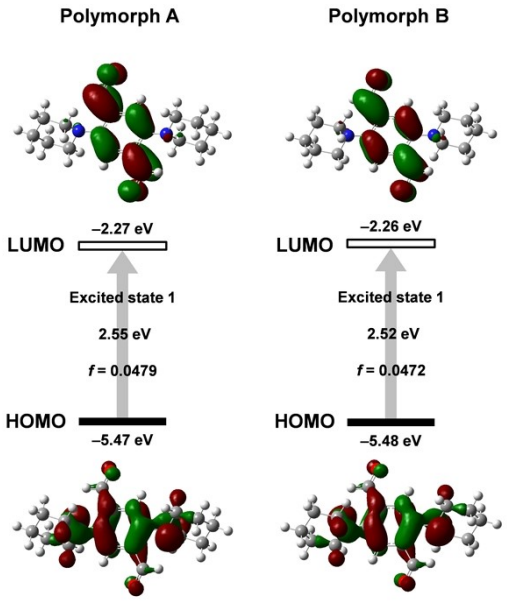


**Figure S3**. TD-DFT calculation results of polymorph A and polymorph B: energy diagrams, Kohn-Sham HOMOs and LUMOs, vertical excitation energies, and oscillator strengths.

**Table S2.** Optical properties of some crystals of SBFs.

| Organic crystals of SBFs | Name | $\lambda_{em}$ (nm) | $\Phi_F$ / % |
|---|---|---|---|
| **Organic crystal** | **Polymorph B of wx-1 (this work)** | **657** | **12** |
| Organic crystal | 1a[2] | 620 | 40 |
| Organic crystal | 1b[2] | 608 | 31 |
| Organic crystal | 1c[2] | 618 | 39 |
| Organic crystal | 5[3] | 638 | 43 |
| Organic crystal | 1d[4] | 640 | 4 |
| Organic crystal | Polymorph A[5] | 622 | 8 |
| Organic crystal | Polymorph B[5] | 640 | <1 |
| Organic crystal | Form 1[6] | 594 | 5 |
| Organic crystal | Form 2[6] | 622 | 3 |
| Organic crystal | DMCAT-1[7] | 632 | 11 |
| Organic crystal | DMCAT-2[7] | 638 | 17 |
| Organic crystal | 3[8] | 617 | 21 |
| Organic crystal | Form A[9] | 644 | 5 |
| Organic crystal | Form B[9] | 623 | 6 |

**Table S3.** Optical waveguide properties of some crystals of SBFs and polymers

| Organic crystals of SBFs/polymers | Name | $\lambda_{em}$ (nm) | Optical loss coefficients / dB $mm^{-1}$ |
|---|---|---|---|
| Organic crystal | Polymorph B of wx-1 (this work) | 657 | 0.179 |
| Organic crystal | Polymorph A of compound 2[10] | 622 | 0.351 (straight) |
| | | | 0.376 (bended) |
| Organic crystal | 1d@2d[11] | 615 | 0.196 (straight) |
| | | | 0.192 (bended) |
| | | 576 | 0.272 (straight) |
| | | | 0.275 (bended) |
| Organic crystal | MeDHQB-I[12] | 555 | 0.553 |
| Organic crystal | (Z)-N'-((Z)-3,5-dichloro-2-hydroxybenzylidene)-N,N-dimethylformohydrazonamide[5] | 520 | 0.26 (25ºC) |
| | | 510 | 0.32 (95ºC) |
| Organic crystal | DMBDCA[13] | 499 | 0.00120 |
| Organic crystal | 1G[14] | 500 | 0.233 (straight) |
| | | | 0.242 (bended) |
| | 1B[14] | 420 | 0.374 (straight) |
| | | | 0.388 (bended) |
| Polymer | Dow Red F[15] | 685 | 0.32 |
| Polymer | F8BT[15] | 576 | 0.76 |
| Polymer | F8DP[15] | 452 | 1.48 |
| Polymer | DOO-PPV[16] | 630 | 3.0 |
| Polymer | BuEH-PPV[17] | 565 | 4.4 |

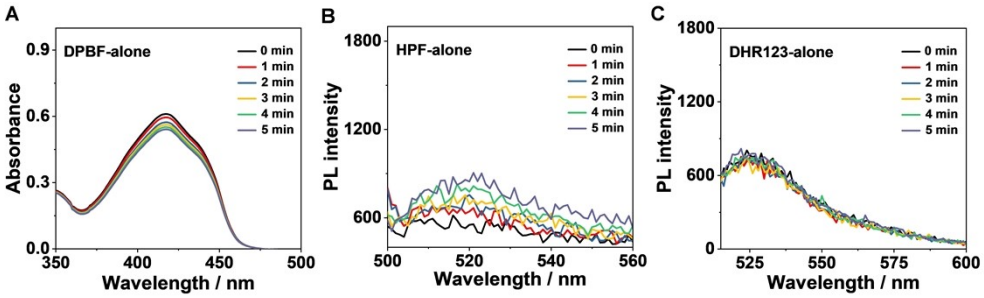


**Figure S4**. The absorbance of DPBF (50 μM), PL spectra of HPF (5 μM) and DHR123 (5 μM) with wx-1 after exposure to white light irradiation for different times. Power: 0.1 W $cm^{-2}$

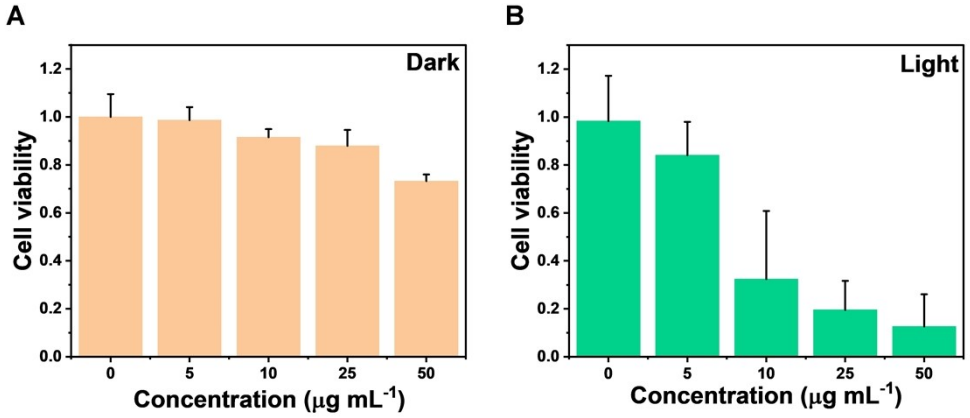


**Figure S5**. (A-B) Viabilities of EMT6 cells incubated with wx-1 exposed to dark or light irradiation (mean ± SD, n = 3).

## 14. NMR Spectra of Synthesized Molecules

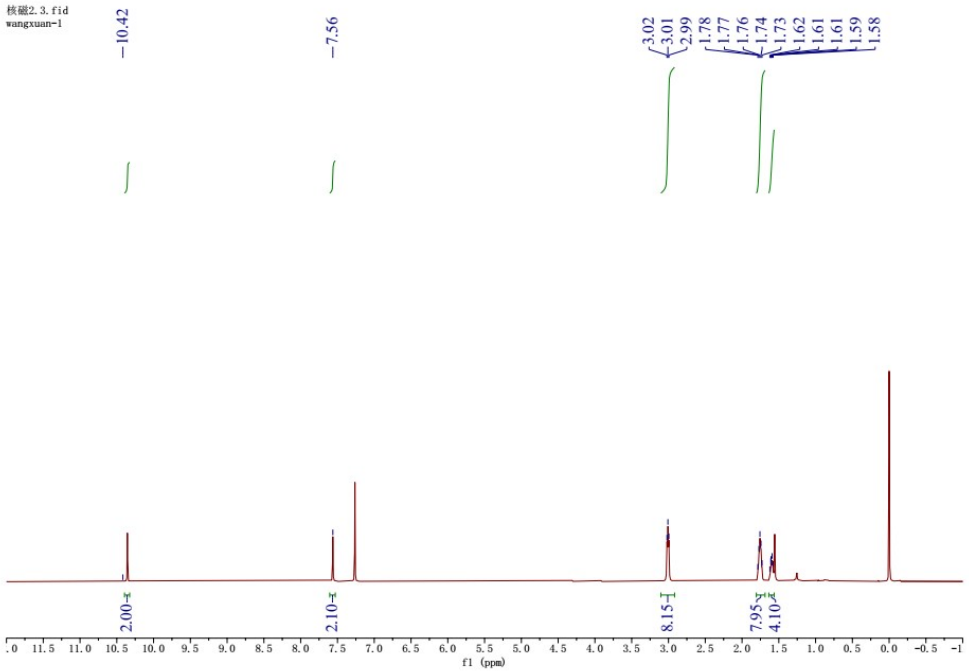


**Fig. S5.** $^{1}$H NMR spectrum of wx-1.

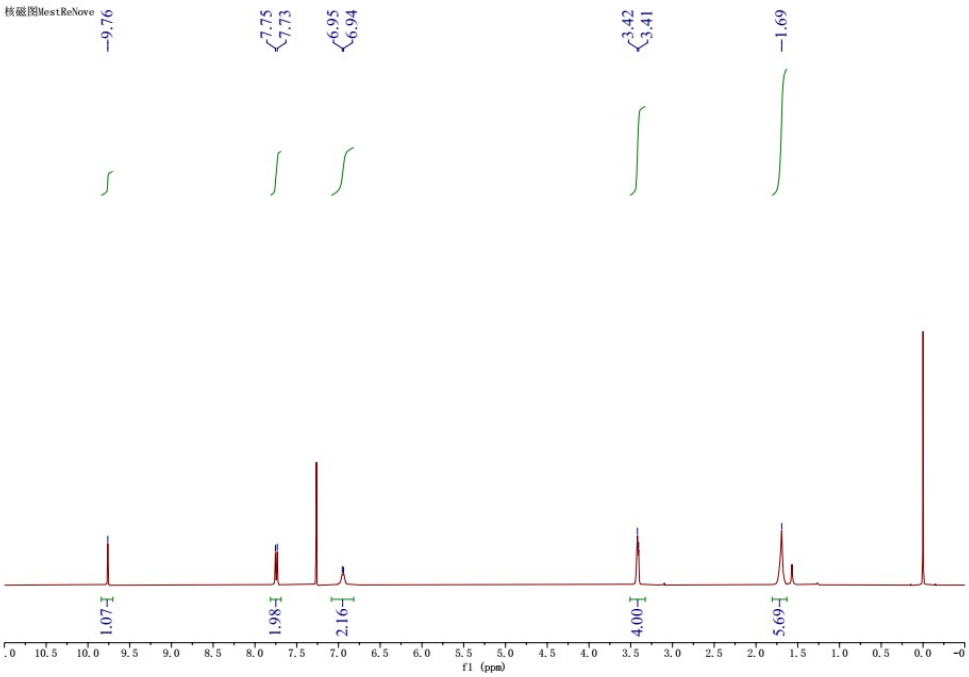


**Fig. S6.** $^{1}$H NMR spectrum of wx-2.

## 15. References


1. K. Hasan, R. G. Joseph, I. A. Shehadi and S. P. Patole, $Fe_3O_4$-chitosan immobilized Cu(II) Schiff base catalyst for the microwave-assisted amination of aryl halides in water, *Arab. J. of Chem.*, 2023, 16, 105317.
2. B. Tang, C. Wang, Y. Wang, H. Zhang, Efficient Red-Emissive Organic Crystals with Amplified Spontaneous Emissions Based on a Single Benzene Framework*, Angew. Chem. Int. Ed.* 2017, 56, 12543-12547.
3. M. Shimizu, Y. Takeda, M. Higashi, T. Hiyama, 1,4-Bis(alkenyl)-2,5-dipiperidinobenzenes: Minimal Fluorophores Exhibiting Highly Efficient Emission in the Solid State*, Angew. Chem. Int. Ed.* 2009, 48, 3653-3656.
4. J. N. Zhang, H. Kang, N. Li, S. M. Zhou, H. M. Sun, S. W. Yin, N. Zhao, B. Z. Tang, Organic solid fluorophores regulated by subtle structure modification: color-tunable and aggregation-induced emission*, Chem. Sci.* 2017, 8, 577-582.
5. B. Liu, Q. Di, W. Liu, C. Wang, Y. Wang, H. Zhang, Red-Emissive Organic Crystals of a Single-Benzene Molecule: Elastically Bendable and Flexible Optical Waveguide*, J. Phys. Chem. Lett.* 2019, 10, 1437-1442.
6. X. Zhang, J. Wang, H. Liu, F. Yu, T. Wang, X. Huang, H. Hao, Polymorphism-dependent fluorescent emission, acid/base response and selective fluorescent sensor for Cu2+ ions based on single-benzene framework*, Dyes Pigm.* 2022, 197, 109903.
7. F. Yu, X. Zhang, H. Zhao, Z. Jiang, T. Wang, N. Wang, X. Huang, L. Zhou, H. Hao, Enhanced luminescence of single-benzene fluorescent molecules through halogen bond cocrystals*, CrystEngComm* 2022, 24, 3537-3545.
8. B. Tang, S. Tang, C. Qu, K. Ye, Z. Zhang, H. Zhang, Side-Chain Engineering of Organic Crystals for Lasing Media with Tunable Flexibility2023, 5, 2348-2357.
9. L. Lan, Q. Di, L. Li, B. Liu, X. Yu, P. Naumov, H. Zhang, Packing-Dependent Mechanical Properties of Schiff Base Crystals*, Crystal Growth & Design* 2022, 22, 3435-3441.
10. R. Huang, C. Wang, Y. Wang and H. Zhang, Elastic Self-Doping Organic Single Crystals Exhibiting Flexible Optical Waveguide and Amplified Spontaneous Emission, *Adv. Mater.*, 2018, 30, 1800814.
11. X. Zhang, J. Wang, H. Zhao, Z. Jiang, K. Chen, T. Wang, X. Huang, N. Wang and H. Hao, Efficient single benzene AIE system: Optical waveguide and invisible ink, *Dyes Pigm.*, 2023, 209, 110947.
12. B. Liu, Z. Lu, B. Tang, H. Liu, H. Liu, Z. Zhang, K. Ye and H. Zhang, Self-Waveguide Single-Benzene Organic Crystal with Ultralow-Temperature Elasticity as a Potential Flexible Material, *Angew. Chem. Int. Ed.*, 2020, 59, 23117-23121.
13. S. Hayashi, T. Koizumi and N. Kamiya, 2,5-Dimethoxybenzene-1,4-dicarboxaldehyde: An Emissive Organic Crystal and Highly Efficient Fluorescent Waveguide, *CHEMPLUSCHEM*, 2019, 84, 247-251.
14. B.-l. Tang, X. Yu and H.-y. Zhang, Supramolecular Polymorphic Crystals with Luminescence and Elasticity Based on a Single Benzene Framework, *Acta Polym.*

*Sin.,* 2021, 52, 1015-1023.
15. R. D. Xia, G. Heliotis and D. D. C. Bradley, Fluorene-based polymer gain media for solid-state laser emission across the full visible spectrum, *Appl. Phys. Lett.*, 2003, 82, 3599-3601.
16. S. V. Frolov, Z. V. Vardeny and K. Yoshino, Cooperative and stimulated emission in poly($p$-phenylene-vinylene) thin films and solutions, *Phys. Rev. B*, 1998, 57, 9141-9147.
17. M. D. McGehee, R. Gupta, S. Veestra, E. K. Miller, M. A. A Díaz-García and A.J. Heeger, Amplified spontaneous emission from photopumped films of a conjugated polymer, *Phys. Rev. B*, 1998, 58, 7035-7039.